THE JOURNAL OF PHYSICAL CHEMISTRY B

Article

pubs.acs.org/JPCB

# NMR Relaxation in Proteins with Fast Internal Motions and Slow Conformational Exchange: Model-Free Framework and Markov State Simulations

Junchao Xia, Nan-jie Deng, and Ronald M. Levy*

Department of Chemistry and Chemical Biology and BioMaPS Institute for Quantitative Biology, Rutgers, the State University of New Jersey, 610 Taylor Road, Piscataway, New Jersey 08854, United States

Supporting Information

**ABSTRACT:** Calculating NMR relaxation effects for proteins with dynamics on multiple time scales generally requires very long trajectories based on conventional molecular dynamics simulations. In this report, we have built Markov state models from multiple MD trajectories and used the resulting MSM to capture the very fast internal motions of the protein within a free energy basin on a time scale up to hundreds of picoseconds and the more than 3 orders of magnitude slower conformational exchange between macrostates. To interpret the relaxation data, we derive new equations using the model-free framework which includes two slowly exchanging macrostates, each of which also exhibits fast local motions. Using simulations of HIV-1 protease as an example, we show how the populations of slowly exchanging conformational states as well as order parameters for the different states can be determined from the NMR relaxation data.

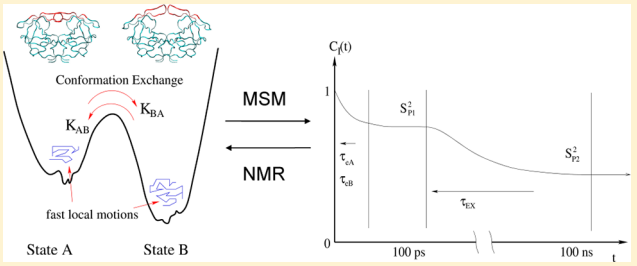


## INTRODUCTION

The study of the dynamics of proteins can help us to understand the mechanisms of molecular recognition which underly such processes as ligand binding, allosteric inhibition, and signaling.[1,2] Human immunodeficiency virus type 1 protease (HIV-1 PR) is an enzyme involved in the processing of gag-pol polyproteins, a critical step for the viral maturation and the life cycle of HIV-1. Many X-ray crystal structures[4] of HIV-1 PR have been solved both in the free state and in complex with inhibitors. The free state (e.g., PDB 1HHP), without inhibitors bound, is defined by a semiopen conformation which is a $C_2$-symmetric homodimer with a substrate-binding pocket loosely covered by two $\beta$-hairpins (the flaps). When complexed with inhibitors (e.g., PDB 1HVR), however, HIV-1 PR has a closed form. Namely, the two flaps close in toward the bottom of the active binding site and form a complete cavity closure; in addition, there is a change in the relative orientation of the flaps (i.e., change in "handedness"). To accomplish ligand binding, it is thought that the two flaps have to open further to allow for access of the ligand to the active site.[5] Such an open state (PDB 1TW7) was found in a crystal structure which was determined to be stabilized by crystal packing contacts.[6] (See Figure 1 for pictures of the four macrostates of HIV-1 PR.)

Obtaining dynamical information for HIV-1 PR in solution, however, requires resorting to other techniques, such as nuclear magnetic resonance (NMR) relaxation R1/R2/NOE,[7−9] chemical exchange from Carr−Purcell−Meiboom−Gill (CPMG) and spin-lock experiments,[10] and electron paramagnetic resonance (EPR) experiments.[11] Through measurements of R1/R2/NOE, the Torchia group found that residues in the flap tips are flexible on the sub-nanosecond time scale.[9] Chemical exchange experiments,[10] however, showed that the flaps undergo significant rearrangement from the semiopen to the closed state on a much longer time scale of up to 100 $\mu$s. Typically, NMR relaxation parameters (R1/R2/NOE) have been used to probe sub-nanosecond fast motions,[12,13] because the application of the popular model-free approach[14,15] to their interpretation requires that the internal motions be separated from overall rotations and decay on a much faster time scale than the tumbling. In contrast, chemical exchange effects probed by CPMG and spin-lock experiments[16] detect much slower motions on the micro- to millilsecond time scale associated with larger conformation changes. These transitions are typically modeled as occurring between macrostates (free energy basins) which lack internal motion, e.g., they are assumed to be rigid. In this paper we provide a framework for extracting information from NMR relaxation measurements (R1/R2/NOE) about the populations of interconverting macrostates which also undergo fast motions within the macrostates. We show how the model-free approach to extract order parameters for fast motions within a single macrostate can be extended to include fast motions within two (or more) macrostates and the much slower conformational exchange between them. The expression for the NMR relaxation simplifies in two limits: when the conformational exchange is

**Received:** January 23, 2013
**Revised:** May 1, 2013

   dx.doi.org/10.1021/jp400797y | J. Phys. Chem. B XXXX, XXX, XXX−XXX

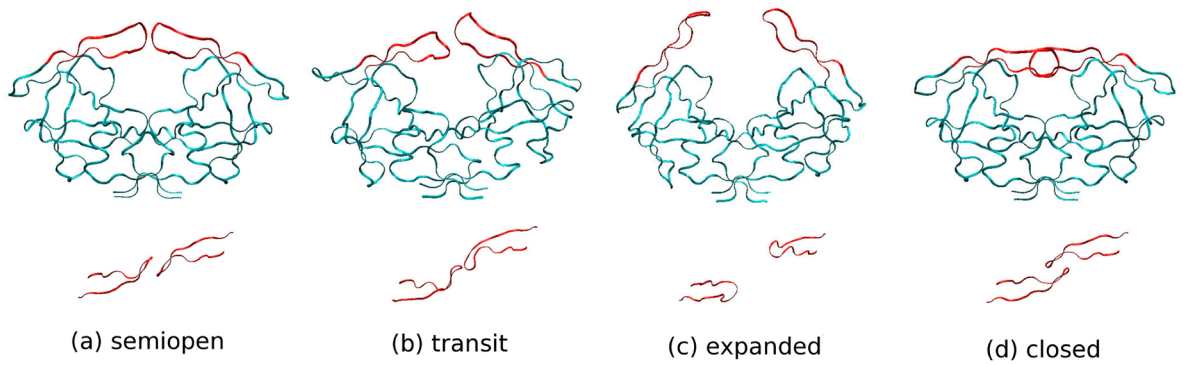


**Figure 1.** Four macrostates of HIV-1 PR from crystal structures and our MD simulation with the OPLS-AA force field and the AGBNP implicit solvent model (top, side views; bottom, top views of flaps only): (a) semiopen crystal structure (PDB 1HHP), (b) transit state from MD simulation (RMSD from the semiopen is 2.61), (c) expanded state (similar to PDB 1TW7) from MD simulation (RMSD from the semiopen is 6.47), and (d) closed crystal structure (PDB 1HVR without ligand; RMSD from the semiopen is 3.26). Residues 51 and 52 are located in the tip of each flap.

much slower than the tumbling (the common situation) or much faster than the tumbling.

Many molecular dynamics (MD) simulations[6,17−27] of HIV-1 PR have been performed, and the general picture that emerges is consistent with experimental results, although the transition time scales between macrostates estimated from MD results are much faster than experiments suggest.[10] The unliganded HIV-1 PR in solution predominantly occupies a semiopen macrostate, and there is also a closed state component.[17−19,22,28] The transition between the semiopen state and the closed state can be achieved through large conformational rearrangements of the two $\beta$-sheet flaps and may also involve other intermediates such as the transient open state.[6,16−19,24] A major drawback of standard MD simulations is that the current computer power limits the time scales that can be simulated to values where only a very small number of slow conformational changes on times of the order of microseconds can be observed, and therefore the ability to converge quantities like NMR correlation functions for the internal motions is severely compromised. Early simulations only lasted from a few hundred picoseconds[28] to several nanoseconds.[18,19] Simmerling's group utilized an implicit solvent model[29] and extended the time scale to ∼40 ns.[22,23] More recent reports[25] have included explicit waters and reached 100 ns. The latest GPUGRID project (http://gpugrid.net) performed large ensembles (461) of explicit solvent MD simulations each with an average simulation time of 50 ns.[26]

To reach simulations lasting tens of microseconds or longer in a single trajectory, we have to resort to either special purpose computers such as Anton from the Shaw research group[30,31] or more advanced simulation methods.[17,20,21,27,28,32] Coarse-grained models[20,21] reduce an atomic residue to one bead and enable dynamical simulations on the time scale of tens of microseconds, but with the sacrifice of atomic details and the elimination of all fast modes, which may be important for modeling the motions of larger protein segments like the HIV PR flaps. Accelerated MD simulations such as metadynamics[32] have been performed to study the substrate binding mechanism of HIV-1 PR using a 1.6 $\mu$s trajectory with explicit solvent. Although accelerated methods are able to locate free energy minima and construct free energy surfaces on a shorter simulation time scale than standard MD methods, the real dynamics of conformational changes is difficult to recover. Furthermore, many accelerated methods require a predefinition of reaction coordinates and are limited to problems in low dimensions. To obtain protein folding trajectories on the time scale of microseconds, recently our group[33−36] developed a framework using Gillespie stochastic simulations[44] based on Markov state models[37−41](MSMs) that were constructed from atomistic replica exchange molecular dynamics (REMD) simulations.[42−44] We were able to generate microsecond trajectories for HIV-1 PR at six different temperatures, compute transition pathways between different native forms of HIV-1 PR, and determine key features of the kinetics without specifying the reaction coordinates in advance.[27]

In principle NMR relaxation parameters can be calculated directly by analyzing MD trajectories,[45−48] although doing so requires very long simulations, at least an order of magnitude longer than the slowest decay of the motions of interest. Trajectories of tens of microseconds or longer durations are needed to capture the effects of slow conformational exchange on NMR parameters.[49−56] In this report we use MSMs[37−41] to generate stochastic trajectories lasting 10 $\mu$s for HIV-1 PR, and we compute the corresponding NMR correlation functions. We show how the results can be interpreted using a model-free framework that includes fast internal motions coupled with slow conformational exchange.

## THEORY AND METHODS

**Building the Markov State Kinetic Network Model.** Recently, MSMs[37−41,56−58] have been constructed to study the complex dynamics of proteins on long time scales, including larger scale conformational transitions,[27,60,61] protein folding,[33,36,43,62,63] and ligand binding.[32,64] In these models the conformational space is discretized onto a set of states, and a network connecting them is constructed from short time MD simulations, for example. The construction of a transition matrix to connect the states is crucial; it can be constructed from an energy-landscape approach[41,65] based on the energy minima and first-order saddle points, from a dynamical approach utilizing short[66,67] or long MD simulations[62] and Bayesian techniques,[63,68−70] or by utilizing REMD[42] and constructing links based on structural similarity.[27,33,35,36] In a previous study[27] of the kinetics of HIV-1 PR using a MSM, we analyzed pathways for opening the flaps of HIV-PR at different temperatures using transition path theory. In this report we build a kinetic network at finer resolution and compute NMR relaxation effects from the stochastic trajectories on the network.

The details regarding the MD simulations of HIV-1 PR dimer, the construction of the kinetic network, and the


dx.doi.org/10.1021/jp400797y | J. Phys. Chem. B XXXX, XXX, XXX−XXX

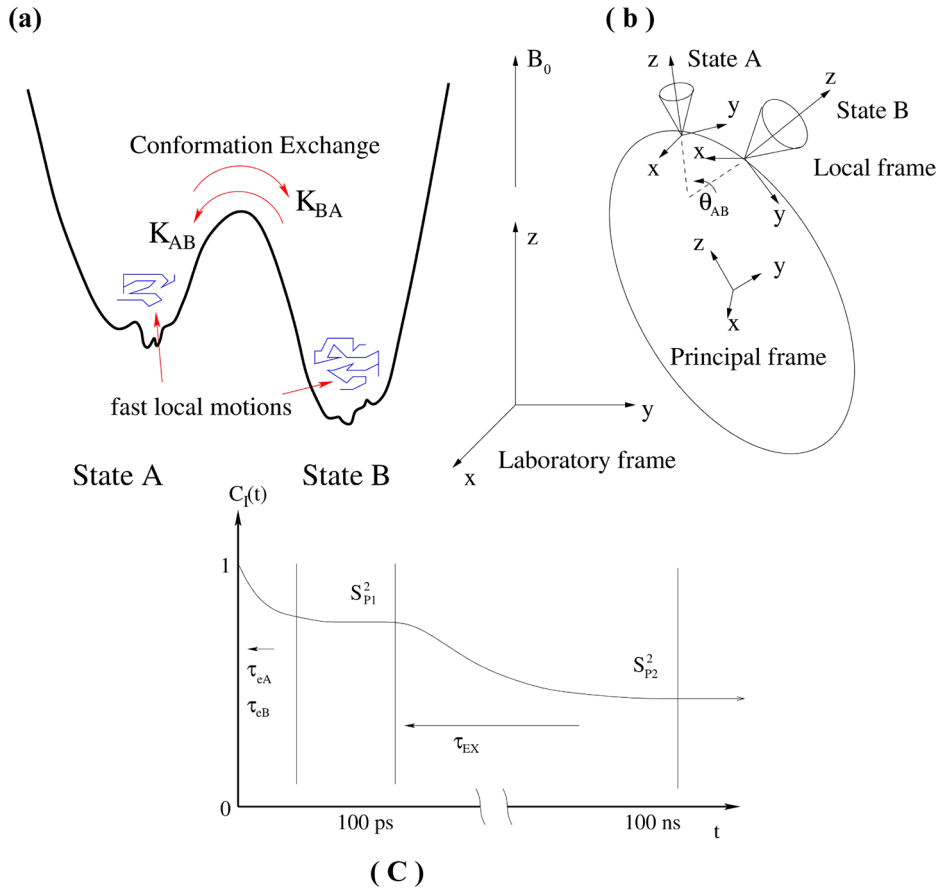


**Figure 2.** Two-state conformation exchange model. The macromolecule has two distinct conformation states A and B which share the same principal coordinates frame (diffusion tensor). (a) Free energy representation, (b) motions represented by different coordinate frames, and (c) schematic graph for a rotational correlation function of internal motions.

stochastic simulation are described in our previous work[27,33,36] and the Supporting Information (SI). Briefly, 20 MD simulations of HIV-1 PR, each of duration 20 ns, were performed using the molecular simulation package IMPACT[71] with the OPLS-AA force field (2005)[72] and the AGBNP implicit solvent model.[73,74] To build the network, we first chose 200 000 snapshots which were stored every 2 ps from the 20 MD trajectories each of length 20 ns, and then calculated the C-$\alpha$ RMSD matrix for both flaps (residues 43−58 and 142−157) between each pair of snapshots, which requires storage of $4 \times 10^{10}$ matrix elements. These snapshots were clustered into 82 291 conformational nodes using an RMSD criterion of 0.5 Å, and each node has a corresponding snapshot. (See Figure S3 in the SI for the distributions of these clustered nodes, the classification of these nodes to four macrostates, and the positions of four macrostates when they are projected onto the first two principal components.) The kinetic network of conformational nodes was created by connecting all pairs of nodes which have node snapshot RMSDs < 1.2 Å. The rate constant $k_{ij}$ between any two connected nodes was parametrized to fit the short time molecular dynamics using eq 6 in the SI. The key idea is that large conformational changes are propagated by many local transitions through structurally similar nodes. This assumption is reasonable when the resolution of the network model is high; in a high-resolution network the local kinetics on the network is largely diffusive, and large-scale conformational kinetics are determined by a combination of local diffusive motions and the varying density of the network nodes along the transition paths, which determines the probability of being at a barrier. We note that this approach is similar in spirit to the method of estimating the rate matrix from metadynamics trajectory data by Laio et al.,[32,91] except that in our approach the MD is not biased along predetermined reaction coordinates. A 10 $\mu$s trajectory was generated from the Gillespie stochastic simulation[44] on the kinetic network starting from a node in the semiopen state.

**Two-Macrostate Exchange Model with Internal Motion for NMR Relaxation.** For a molecule with a single free energy minimum significantly lower than all the others, the model-free approach[14] and its extended version[15] are the main theoretical frameworks used to estimate structural and dynamical information from NMR fast relaxation experiments by neglecting the other free energy basins. Namely, the global free energy minimum defines a macrostate, and the fast local fluctuations around the minimum are sufficient to explain NMR relaxation quantities such as R1/R2/NOE. Due to its simplicity and generality, the model-free framework is the main way that NMR fast relaxation measurements on proteins are analyzed,[8,9] with the diffusion tensor describing the overall rotation and the order parameter $S^2$ and decay constant $\tau_e$ representing local internal motions of each residue that can be fitted from the experimental values of R1/R2/NOE. This framework, however, will fail if there exist large conformational changes to other macrostates and the populations of the other states are not substantially smaller than the major one. For the case of HIV-1 PR, previous analysis based on this model-free framework could


dx.doi.org/10.1021/jp400797y | J. Phys. Chem. B XXXX, XXX, XXX−XXX

not provide distinct values for the populations of the semiopen and closed states.[8,9]

To extract the populations of two macrostates and information about their fast internal motions and slow conformational exchange from NMR relaxation experiments, we have derived general equations for the rotational correlation functions of spin−spin vectors using a model which includes these effects. The results for the two-state exchange model between free energy basins which also includes fast internal motions within each basin as depicted in Figure 2 are presented below. Assuming the existence of a common diffusion tensor and the exchange time is well-defined between two states which can be described locally by the model-free approach,[14] we found that the internal rotational correlation function of a spin−spin vector can be written as follows (see eqs 35−37 in the SI):

$$C_I(t) = S^2(t) + [F(t) - S^2(t)]\, e^{-t/\tau_{EX}} \quad (1)$$

with

$$S^2(t) = P_A^2 S_A^2 + 2P_A S_A P_B S_B P^{(2)}(\cos\theta_{AB}) + P_B^2 S_B^2 + P_A^2(1 - S_A^2)\, e^{-t/\tau_{eA}} + P_B^2(1 - S_B^2)\, e^{-t/\tau_{eB}} \quad (2)$$

and

$$F(t) = P_A S_A^2 + P_B S_B^2 + P_A(1 - S_A^2)\, e^{-t/\tau_{eA}} + P_B(1 - S_B^2)\, e^{-t/\tau_{eB}} \quad (3)$$

As shown in Figure 2, the correlation function converges to three important values on different time scales (see eqs 40−42 in the SI):

$$C_I(t) = P_A + P_B = 1, \quad t \to 0 \quad (4)$$

$$S_{P1}^2 = C_I(t) = P_A S_A^2 + P_B S_B^2, \quad \tau_{eB}(\tau_{eA}) \ll t \ll \tau_{EX} \quad (5)$$

$$S_{P2}^2 = C_I(t) = P_A^2 S_A^2 + 2P_A S_A P_B S_B P^{(2)}(\cos\theta_{AB}) + P_B^2 S_B^2, \quad t \to \infty \quad (6)$$

where $P_A$ ($P_B$), $S_A^2$ ($S_B^2$), and $\tau_{eA}$ ($\tau_{eB}$) denote the equilibrium populations, generalized order parameters, and time constants of internal motions from the model-free theory for the two distinct macrostates (A and B, respectively), and $\theta_{AB}$ is the angle between the two equilibrium positions of a spin−spin vector in state A and state B. $P^{(2)}(x)$ is the second-order Legendre polynomial. $\tau_{EX}$ is the time constant of two-state exchange which is related to the two rate constants (A →B and B→A) by $\tau_{EX} = 1/(k_{AB} + k_{BA})$. After multiplying the overall rotation and internal correlation functions (eqs 45 and 46 in the SI) and Fourier-transforming, eqs 1−6 provide a new way to extract equilibrium and dynamics information for the individual macrostates and the exchange rate between them from NMR relaxation data.

Which equation (eq 5 or 6) to fit the data to depends on the relative time scales of overall rotation $\tau_M$ ($\tau_1$, $\tau_2$, and $\tau_3$ for anisotropic cases) and conformational exchange $\tau_{EX}$. When $\tau_e \ll \tau_M \ll \tau_{EX}$ (slow exchange model), the decay of overall rotation is much quicker than the rate of exchange between the two macrostates, $C_I(t) \to F(t)$, and the second plateau eq 6 is averaged out by the tumbling. In contrast, both plateaus, eqs 5 and 6, contribute in the fast exchange limit when $\tau_M \gg \tau_{EX} \gg \tau_e$.

## RESULTS AND DISCUSSION

**Constructing a 10 μs Trajectory from the Kinetic Network Model.** A 10 μs trajectory was obtained from the stochastic simulations on the kinetic network constructed from 20 short MD trajectories each of length 20 ns (see section 1 in the SI). A total of 3 123 612 conformational snapshots were saved for analysis once a transition to new node occurs. (Note that snapshots are not evenly distributed for a Gillespie simulation.) In Figure 3, we display the RMSD time series of the two flaps by aligning all conformational snapshots to the

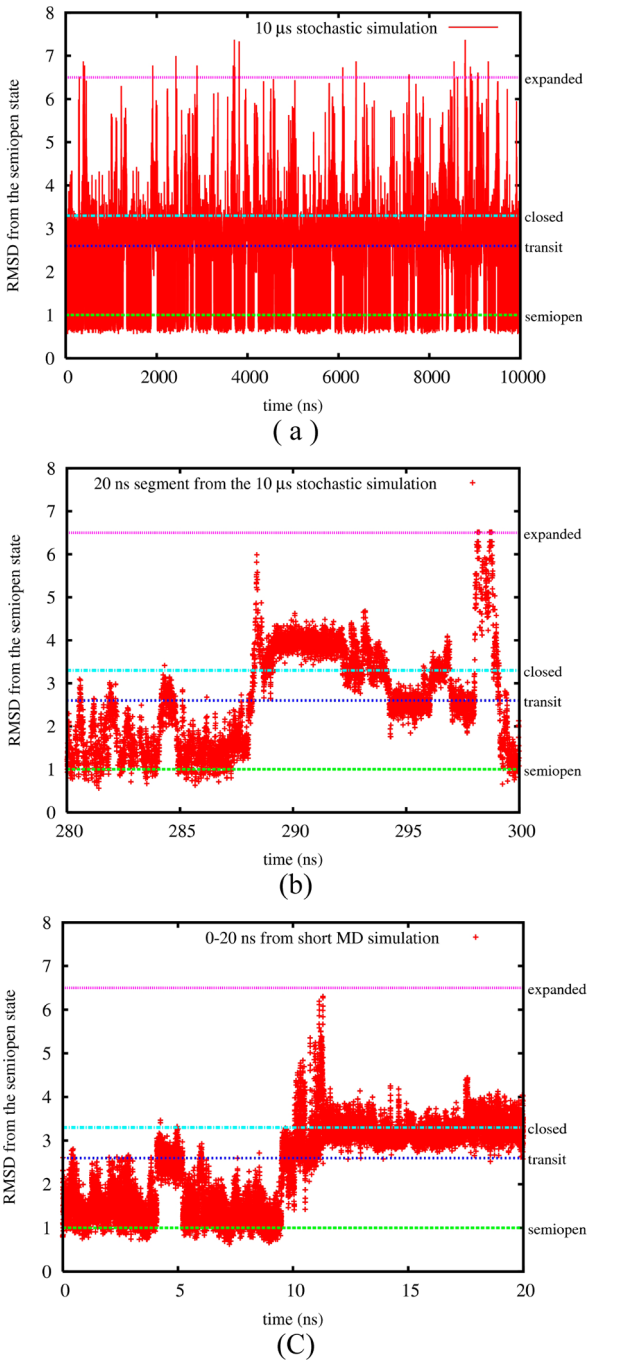


**Figure 3.** Time series of RMSDs from the semiopen crystal state in different simulation trajectories. The color lines mark the RMSDs of four states in Figure 1. (a) 10 μs network simulation, (b) 280−300 ns part of (a), and (c) 20 ns from one of the short MD simulations.


dx.doi.org/10.1021/jp400797y | J. Phys. Chem. B XXXX, XXX, XXX−XXX

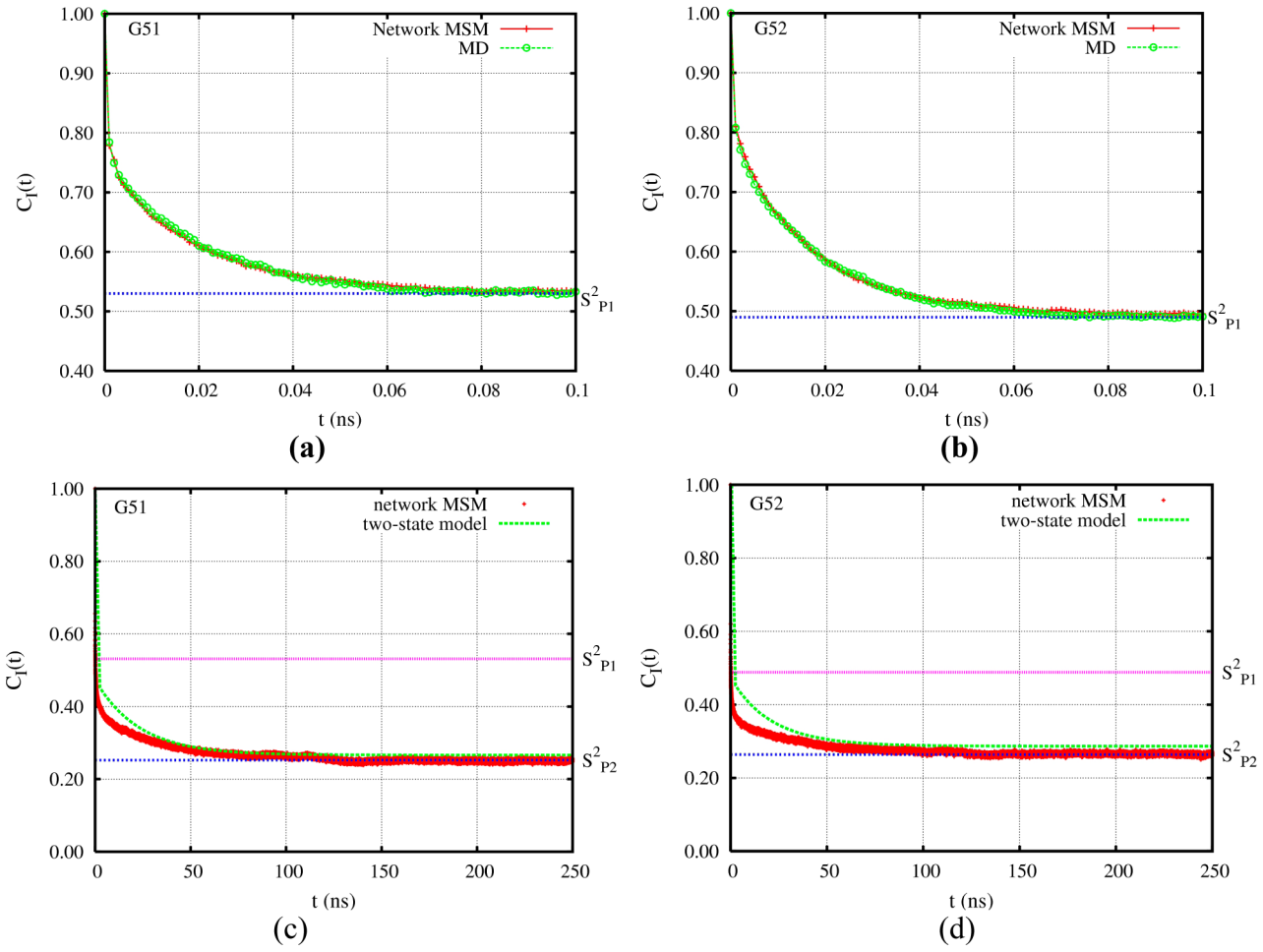


**Figure 4.** Comparison of internal correlation functions of the N−H vectors from residue 51 and 52: (a,b) correlation functions of residue 51 and 52 at first 100 ps from the network MSM and that from the 20 ns MD trajectories; (c,d) correlation functions of residue 51 and 52 up to 250 ns from the network MSM and the theoretical prediction of two-macrostate slow exchange model with fast internal motion (eqs 1−3). The color lines mark the calculated $S^2_{P1}$ and $S^2_{P2}$ from the network MSM.

semiopen crystal state (PDB 1HHP). The trajectory starts from a conformational node in the semiopen state and experiences 79 transition events from the semiopen to the closed conformation, and from the closed to semiopen state respectively. The mean first passage time for the former is 95.0 ns and 30.8 ns for the latter and results in an estimated exchange time of 23.3 ns. This result is consistent with our previous work,[20] where the kinetic network was built from REMD conformations sampled at different temperatures and weighted to the target temperature using the T-WHAM method.[75]

The transition time scale (∼100 ns) from the semiopen to the closed state is consistent with other simulation results.[22,25−27] However, it is apparently much faster than the experimentally estimated relaxation time which is of the order of 70 $\mu$s.[10] This discrepancy might be due to two factors, one experimental and the other computational. The measured chemical shift differences used to extract the transition time scale from the CPMG experiment[10] may correspond to the differences between the semiopen state and the expanded one (with smaller population and longer exchange time[27]) instead of the differences between the semiopen and the closed state. Second, the discrepancy may be due to the protein force field and the use of an implicit solvent model which does not include the frictional effects of the solvent on the motion. Early MD simulations[18,19,28] were able to observe the flap opening from the semiopen state (e.g., the semiopen to the transit state in Figure 3) but not the transition to the closed state. Recently the Simmerling group[22] found a transition of the semiopen to the closed state within 10 ns using the AMBER FF99 force field[76] and the implicit (Generalized Born) model[29] with low viscosity, but no transitions within 45 ns with the addition of explicit waters. More recent simulations[25] with the AMBER FF99 and TIP3P explicit water model exhibited one transition on the 100 ns time scale. We emphasize that our 10 $\mu$s MSM trajectory provides many more observations of transitions in a series from the semiopen to transit, to expanded, and back to the closed state than previous simulations.

The colored lines in Figure 3 mark four states shown in Figure 1. Also shown in Figure 3 are a 20 ns segment (Figure 3b) from the MSM trajectory and a 20 ns segment (Figure 3c) from the MD trajectory respectively. The MSM and MD trajectories exhibit very similar behavior. The semiopen and the closed states have longer lifetimes than the other two metastable states. The transit state is a metastable intermediate with a short lifetime (several nanoseconds). The expanded state is visited after the transit state and has the shortest lifetime compared with the other three (less than 1 ns).

**Correlation Functions and NMR Parameters from the Network MSM Trajectory.** Figure 4 shows the internal


dx.doi.org/10.1021/jp400797y | J. Phys. Chem. B XXXX, XXX, XXX−XXX

rotational correlation functions and plateaus on different time scales (the first 100 ps and up to 250 ns) for the N−H vectors of residues 51 and 52, computed from the 10 $\mu$s network MSM trajectory. (More correlation functions of residues in the floppy flap regions are included in Figures S4 and S5.) From these figures, we can see that the correlation functions for some residues (e.g., 40, 47, and 60) decay and reach the plateau value ($S^2_{P2}$, equilibrium $S^2$ ($C_I(\infty)$)) very quickly, on a time scale of picoseconds. For other residues (e.g., 49, 50, 51, and 52) instead, the correlation functions have a very quick initial decay (picoseconds) to an initial plateau ($S^2_{P1}$) and then a slow decay on a much longer time scale, ∼100 ns, gradually approaching the second plateau value ($S^2_{P2}$). The time scales for the slow decay are close to the mean first passage time of the transition from the semiopen to closed state.

As shown in Figure 4a,b, the fast decays of the rotational correlation functions for residues 51 and 52 (on the flap tip) during the first 100 ps calculated from the Markov state network simulations agree well with those from the underlying MD simulations. Namely, the local dynamics within the macrostates sampled by the MD simulations are captured by the network MSM. Figure S6 shows that the equilibrium order parameters $S^2$ ($S^2_{P2}$ from the average of all snapshots) calculated from the 20 MD simulations (20 ns per simulation) are consistent with those from the 10 $\mu$s network MSM trajectory. The agreement between correlation functions and order parameters calculated from the MD simulations and those calculated from the stochastic simulations on the kinetic network confirms that the construction of the network and the stochastic simulations capture the main characteristics of the fast local dynamics of the individual macrostates and the slow semiopen to closed state transition. Furthermore, as shown in Figure S7, the calculated order parameters are qualitatively consistent with those derived from the NMR experiments,[9] except that residues 51 and 52 appear less flexible when comparing the order parameters derived from the experimental NMR relaxation data with the values extracted from the MSM simulation. We should note that the residue 51 and 52 are located in the tips of two flaps and exhibit more complicated motions comparing to other residues. The experiment derivation,[9] instead, only used a model-free model assuming a single free energy minima.

Figure 4c,d compares the rotational correlation functions for residues 51 and 52 calculated from the 10 $\mu$s network MSM trajectory with the theoretical predictions from the two-macrostate model (with fast internal motions) of eqs 1−3 using the $S^2$ values of the semiopen and closed states in Figure 5, the populations fitted in Figure 6b, and the exchange time of 23.3 ns. The theoretical curve of residue 51 overlaps with the one calculated directly from the network MSM very well. The prediction for residue 52 is slightly worse than that of residue 51. This is mostly due to the fact that $S^2_{P2}$ is sensitive to the cross term in eq 6, which is determined by the average angle of the spin vectors between the equilibrium positions of the semiopen and closed states. The agreement can be improved if the spin vector equilibrium positions of both states are allowed to optimize.

**Fitting the Model-Free Equations to the Markov State Simulation.** Figure 5 displays the order parameters at long time ($S^2 = S^2_{P2} = C_I(\infty)$) calculated from the equilibrium average over the network MSM trajectory for two different macrostates: semiopen and closed, with statistical populations of 0.638 and 0.224. (Figure S8 also includes the transit and

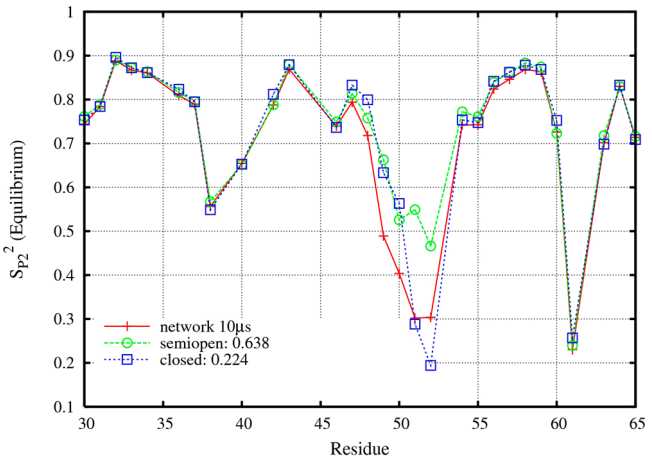


**Figure 5.** $S^2$ ($S^2_{P2} = C_I(\infty)$) for all states, and two different macrostates (semiopen and closed) of HIV-1 PR, calculated from the 10 $\mu$s network trajectory. $S^2_{P2}$ is calculated using the equilibrium average of all snapshots or that belonging to the individual states. The legends in the figure also show the statistical populations (0.638, 0.224) of the two different states. There are other states not belonging to any twos with a total population of roughly 0.14.

expanded states with much smaller populations of 0.012 and 0.001. Note that adding the four populations does not sum to 1.0; there is a residual population of ∼14% which does not correspond to well-defined states.) The semiopen state is the major population and together the semiopen plus closed states contain more than 85% of the total population. This is consistent with the results of previous MD simulations[22,26] and experiments.[9] All four states have similar order parameter $S^2$ profiles, except that there are large differences for residues located in the flap regions. Thus, the local motions of residues within the flaps are significantly different within the different macrostates. For residue 52, $S^2$ is 0.2 within the closed state but is almost 0.5 in the semiopen state. It is worth pointing out that the total $S^2$ for some residues (such as 49 and 50) are smaller than the individual values from the semiopen or closed states. This is, in contrast, different for other residues (e.g., residues 51 and 52) whose total $S^2$ are between the values for the individual semiopen and closed states. This difference originates from the cross term in eq 6 and is not contained within the current model-free theory.[14]

Due to the short life times and very small populations of the transit and expanded states, in what follows we focus on fitting the NMR data only to the semiopen and closed states. Figure 6 shows that the order parameters ($S^2_{P1}$ and $S^2_{P2}$) estimated on different time scales can be well fit to the two-state exchange model using eqs 4−6. The population of the seimopen state was found to be 0.73 and 0.76 for $S^2$ fitted to the short (eq 5) and long time (eq 6) behaviors, respectively. Namely $S^2_{P1}$ ($S^2_{P2}$) calculated from the correlation functions on different time scales can be used to predict the correct populations for the semiopen and closed macrostates, which are consistent with the population statistics extracted directly from the network MSM trajectory. The resulting population of the semiopen state from fitting (∼0.74) is ∼10% larger than the population estimated directly from the network MSM as shown in Figure 5. This is due to the fact that ∼14% of the conformations cannot be assigned to any of the four macrostates and these conformations are absorbed into the semiopen state by the fitting.


dx.doi.org/10.1021/jp400797y | J. Phys. Chem. B XXXX, XXX, XXX−XXX

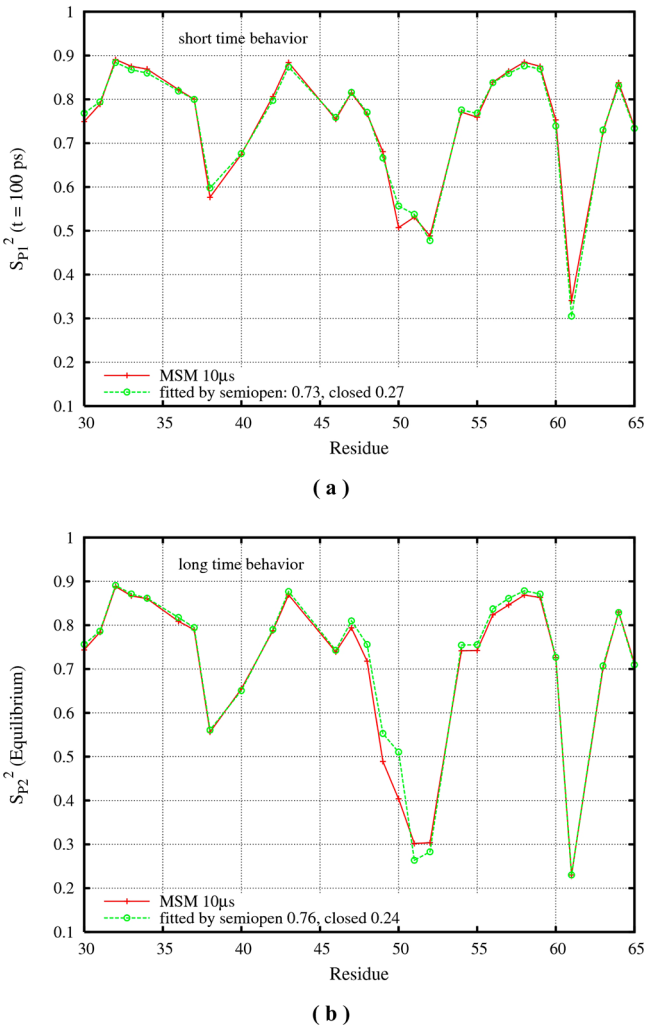


**Figure 6.** $S^2$ from the 10 $\mu$s network trajectory is fitted to two-state exchange model. (a) $S^2_{P1}$ is estimated at $t$ = 100 ps of $C_I(t)$ ($P_A$ = 0.73 and $P_B$ = 0.27 by fitting to eqs 4 and 5). (b) $S^2_{P2}$ is calculated using equilibrium average of all snapshots, and $\theta_{AB}$ is estimated from the simulation data ($P_A$ = 0.76 and $P_B$ = 0.24 by fitting to eqs 4 and 6).

For the analysis presented in this section, the overall tumbling has been removed from consideration, hence we were able to fit $S^2$ on both short and long time scales. Since the experimentally derived time scale of HIV-1 PR isotropic tumbling time[9] in water is around 12 ns, which is much faster than the conformational exchange of the HIIV-1 PR flaps between the semiopen and closed macrostates,[10] in practice, we can only fit experimental data to the slow-exchange model (eqs 4 and 5). For some systems it might be possible to adjust experimental conditions so as to vary the kinetics between the slow and fast exchange limits, e.g., by adjusting the viscosity or temperature to increase the rotational correlation time.

## CONCLUSIONS

In summary, we built a Markov state kinetic network model to study the conformational dynamics of HIV-1 PR using the twenty short MD trajectories (20 ns each) to parametrize the model. The transition matrix among the microstates (network nodes) was estimated using structure similarity rather than Bayesian techniques[63,68−70] In this work, we performed stochastic simulations on the kinetic network and constructed a 10 $\mu$s MSM trajectory to capture the dynamics of the HIV-1 PR flaps. The correlation functions and the NMR order parameters calculated from the stochastic simulation are in accord with the short MD results. Namely, we can build network MSMs from short MD simulations to study not only the short time behavior and local dynamics within the individual states but also capture the long time kinetics corresponding to conformational transitions between macrostates.

Besides the development of early theories[77−81] of NMR relaxation in macromolecules and the introduction of the model-free formula,[14,15] there are other theories which can be used to interpret NMR relaxation in proteins, including those with more complex treatments of the coupling of interdomain and overall motions with different diffusion tensors,[82] the coupling between internal dynamics and rotational diffusion in the presence of exchange,[83,84] and relaxation without separating the overall rotations from internal motions.[85] In this paper we assume the overall and internal motions can be separated and we use the model-free description for the local motions within individual macrostates. We have derived the general equations (see SI) for the rotational correlation functions of spin−spin vectors for a model in which there are two slowly exchanging macrostates, each of which also exhibits fast internal motions. We have demonstrated that the correlation functions derived from this model closely resemble those calculated from the 10 $\mu$s stochastic Markov state trajectory of HIV-1 PR. This suggests that it should be possible to fit the experimental NMR relaxation data of HIV-1 PR to the two-macrostate slow exchange model and extract the local dynamics within the semiopen and closed states as well as the exchange rates between those two states, and their populations. (We should emphasize that the two-state model with fast internal motions within the macrostates is only an approximation to the full dynamics. Such a simple model, though more complicated than the traditional model-free approach, is not expected to reproduce all of the complex dynamics.) Such fitting procedure will help us to understand conformational changes or population shifts of HIV-1 PR due to ligand binding or drug resistant mutation revealed by MD simulations and experiments such as EPR.[86−90] The major problem to be overcome is summarized below.

Generally there are three observables (R1/R2/NOE) for one spin−spin vector from a NMR relaxation experiment with one magnetic field. In contrast, the two-macrostate slow exchange model with fast internal motions requires the determination of five parameters ($S^2_A$, $S^2_B$, $\tau_{eA}$, $\tau_{eB}$, $\theta_{AB}$) for the internal motions of each residue and three parameters ($P_A$, $P_B$, $\tau_{EX}$) for the equilibrium and exchange information which are common to all residues as well as the diffusion tensor for overall motion. Hence the number of experimental data points is smaller than the number of the unknown parameters to fit. In order to tackle this problem, obtaining experimental NMR relation data at multiple magnetic fields is one direction to take. An alternative approach is fitting the experimental quantities from NMR relaxation of HIV-1 PR by simultaneously optimizing the diffusion tensor and the parameters describing the fast internal motions and slow conformational exchange using a genetic algorithm. Work along these lines is underway in our laboratory.


dx.doi.org/10.1021/jp400797y | J. Phys. Chem. B XXXX, XXX, XXX−XXX

## ■ ASSOCIATED CONTENT

### Supporting Information

Details about the building of the Markov state kinetic network, the NMR theory and the derivation of two-state exchange model with fast internal motions, and the calculation of NMR quantities from the trajectories. This material is available free of charge via the Internet at http://pubs.acs.org.

## ■ AUTHOR INFORMATION

### Corresponding Author

*E-mail: ronlevy@lutece.rutgers.edu. Phone: 732-445-3947.

### Notes

The authors declare no competing financial interest.

## ■ ACKNOWLEDGMENTS

This work has been supported by a grant from the National Institutes of Health (GM30580) awarded to R.M.L. MD simulations were carried out on the Gyges cluster at Rutgers supported by NIH shared instrumentation grants nos. S10-RR022375 and S10-RR027444. We thank Emilio Gallicchio for the support of computer resources and for many helpful discussions.

## ■ REFERENCES

(1) Boehr, D. D.; Dyson, H. J.; Wright, P. E. An NMR Perspective on Enzyme Dynamics. *Chem. Rev.* **2006**, *106*, 3055−3079.

(2) Boehr, D. D.; Nussinov, R.; Wright, P. E. The Role of Dynamic Conformational Ensembles in Biomolecular Recognition. *Nat. Chem. Biol.* **2009**, *5*, 789−796.

(3) Hornak, V.; Simmerling, C. Targeting Structural Flexibility in HIV-1 Protease Inhibitor Binding. *Drug Discovery Today* **2007**, *12*, 132−138.

(4) Vondrasek, J.; Wlodawer, A. HIVdb: A Database of the Structures of Human Immunodeficiency Virus Protease. *Proteins: Struct., Funct. Genet.* **2002**, *49*, 429−431.

(5) Martin, P.; Vickrey, J. F.; Proteasa, G.; Jimenez, Y. L.; Wawrzak, Z.; Winters, M. A.; Merigan, T. C.; Kovari, L. C. "Wide-open" 1.3 angstrom Structure of a Multidrugresistant HIV-1 Protease as a Drug Target. *Structure* **2005**, *13*, 1887−1895.

(6) Layten, M.; Hornak, V.; Simmerling, C. The Open Structure of a Multi-drugresistant HIV-1 Protease is Stabilized by Crystal Packing Contacts. *J. Am. Chem. Soc.* **2006**, *128*, 13360−13361.

(7) Nicholson, L. K.; Yamazaki, T.; Torchia, D. A.; Grzesiek, S.; Bax, A.; Stahl, S. J.; Kaufman, J. D.; Wingfield, P. T.; Lam, P. Y. S.; Jadhav, P. K.; et al. Flexibility and Function in HIV-1 Protease. *Nat. Struct. Biol.* **1995**, *2*, 274−280.

(8) Tjandra, N.; Wingfield, P.; Stahl, S.; Bax, A. Anisotropic Rotational Diffusion of Perdeuterated HIV Protease from N-15 NMR Relaxation Measurements at Two Magnetic. *J. Biomol. NMR* **1996**, *8*, 273−284.

(9) Freedberg, D. I.; Ishima, R.; Jacob, J.; Wang, Y. X.; Kustanovich, I.; Louis, J. M.; Torchia, D. A. Rapid Structural Fluctuations of the Free HIV Protease Flaps in Solution: Relationship to Crystal Structures and Comparison with Predictions of Dynamics Calculations. *Protein Sci.* **2002**, *11*, 221−232.

(10) Ishima, R.; Freedberg, D. I.; Wang, Y. X.; Louis, J. M.; Torchia, D. A. Flap Opening and Dimer-Interface Flexibility in the Free and Inhibitor-Bound HIV Protease, and Their Implications for Function. *Structure* **1999**, *7*, 1047−1055.

(11) Galiano, L.; Bonora, M.; Fanucci, G. E. Interflap Distances in HIV-1 Protease Determined by Pulsed EPR Measurements. *J. Am. Chem. Soc.* **2007**, *129*, 11004−11005.

(12) Jarymowycz, V. A.; Stone, M. J. Fast Time Scale Dynamics of Protein Backbones: NMR Relaxation Methods, Applications, and Functional Consequences. *Chem. Rev.* **2006**, *106*, 1624−1671.

(13) Igumenova, T. I.; Frederick, K. K.; Wand, A. J. Characterization of the Fast Dynamics of Protein Amino Acid Side Chains using NMR Relaxation in Solution. *Chem. Rev.* **2006**, *106*, 1672−1699.

(14) Lipari, G.; Szabo, A. Model-Free Approach to the Interpretation of Nuclear Magnetic-Resonance Relaxation in Macromolecules.1. Theory and Range of Validity. *J. Am. Chem. Soc.* **1982**, *104*, 4546−4559.

(15) Clore, G. M.; Szabo, A.; Bax, A.; Kay, L. E.; Driscoll, P. C.; Gronenborn, A. M. Deviations from the Simple 2-Parameter-Free Appoach to the Interpretation of N-15 Nuclear Magnetic-Relaxation of Proteins. *J. Am. Chem. Soc.* **1990**, *112*, 4989−4991.

(16) Palmer, A. G. NMR Characterization of the Dynamics of Biomacromolecules. *Chem. Rev.* **2004**, *104*, 3623−3640.

(17) Rick, S. W.; Erickson, J. W.; Burt, S. K. Reaction Path and Free Energy Calculations of the Transition between Alternate Conformations of HIV-1 Protease. *Proteins: Struct., Funct. Genet.* **1998**, *32*, 7−16.

(18) Scott, W. R. P.; Schiffer, C. A. Curling of Flap Tips in HIV-1 Protease as a Mechanism for Substrate Entry and Tolerance of Drug Resistance. *Structure* **2000**, *8*, 1259−1265.

(19) Meagher, K. L.; Carlson, H. A. Solvation Influences Flap Collapse in HIV-1 Protease. *Proteins: Struct., Funct. Bioinf.* **2005**, *58*, 119−125.

(20) Chang, C. E.; Shen, T.; Trylska, J.; Tozzini, V.; McCammon, J. A. Gated Binding of Ligands to HIV-1 Protease: Brownian Dynamics Simulations in a Coarse-Grained Model. *Biophys. J.* **2006**, *90*, 3880−3885.

(21) Tozzini, V.; Trylska, J.; Chang, C.-e.; McCammon, J. A. Flap Opening Dynamics in HIV-1 Protease Explored with a Coarse-Grained Model. *J. Struct. Biol.* **2007**, *157*, 606−615.

(22) Hornak, V.; Okur, A.; Rizzo, R. C.; Simmerling, C. HIV-1 Protease Flaps Spontaneously Open and Reclose in Molecular Dynamics Simulations. *Proc. Natl. Acad. Sci. U.S.A.* **2006**, *103*, 915−920.

(23) Hornak, V.; Okur, A.; Rizzo, R. C.; Simmerling, C. HIV-1 Protease Flaps Spontaneously Close to the Correct Structure in Simulations Following Manual Placement of an Inhibitor into the Open State. *J. Am. Chem. Soc.* **2006**, *128*, 2812−2813.

(24) Ding, F.; Layten, M.; Simmerling, C. Solution Structure of HIV-1 Protease Flaps Probed by Comparison of Molecular Dynamics Simulation Ensembles and EPR Experiments. *J. Am. Chem. Soc.* **2008**, *130*, 7184−7185.

(25) Li, D.; Ji, B.; Hwang, K.; Huang, Y. Crucial Roles of the Subnanosecond Local Dynamics of the Flap Tips in the Global Conformational Changes of HIV-1 Protease. *J. Phys. Chem. B* **2010**, *114*, 3060−3069.

(26) Kashif Sadiq, S.; De Fabritiis, G. Explicit Solvent Dynamics and Energetics of HIV-1 Protease Flap Opening and Closing. *Proteins: Struct., Funct. Bioinf.* **2010**, *78*, 2873−2885.

(27) Deng, N.-J.; Zheng, W.; Gallicchio, E.; Levy, R. M. Insights into the Dynamics of HIV-1 Protease: A Kinetic Network Model Constructed from Atomistic Simulations. *J. Am. Chem. Soc.* **2011**, *133*, 9387−9394.

(28) Collins, J. R.; Burt, S. K.; Erickson, J. W. Flap Opening in HIV-1 Protease Simulated by Activated molecular-dynamics. *Nat. Struct. Biol.* **1995**, *2*, 334−338.

(29) Tsui, V.; Case, D. A. Theory and Applications of the Generalized Born Solvation Model in Macromolecular Simulations. *Biopolymers* **2000**, *56*, 275−291.

(30) Maragakis, P.; Lindorff-Larsen, K.; Eastwood, M. P.; Dror, R. O.; Klepeis, J. L.; Arkin, I. T.; Jensen, M. O.; Xu, H. F.; Trbovic, N.; Friesner, R. A.; et al. Microsecond Molecular Dynamics Simulation Shows Effect of Slow Loop Dynamics on Backbone Amide Order Parameters of Proteins. *J. Phys. Chem. B* **2008**, *112*, 6155−6158.

(31) Shaw, D. E.; Deneroff, M. M.; Dror, R. O.; Kuskin, J. S.; Larson, R. H.; Salmon, J. K.; Young, C.; Batson, B.; Bowers, K. J.; Chao, J. C.; et al. Anton, a Special-Purpose Machine For Molecular Dynamics Simulation. *Commun. ACM* **2008**, *51*, 91−97.

(32) Pietrucci, F.; Marinelli, F.; Carloni, P.; Laio, A. Substrate Binding Mechanism of HIV-1 Protease from Explicit-Solvent Atomistic Simulations. *J. Am. Chem. Soc.* **2009**, *131*, 11811−11818.
(33) Andrec, M.; Felts, A. K.; Gallicchio, E.; Levy, R. M. Protein Folding Pathways From Replica Exchange Simulations and a Kinetic Network Model. *Proc. Natl. Acad. Sci. U.S.A.* **2005**, *102*, 6801−6806.
(34) Zheng, W.; Andrec, M.; Gallicchio, E.; Levy, R. M. Simulating Replica Exchange Simulations of Protein Folding with a Kinetic Network Model. *Proc. Natl. Acad. Sci. U.S.A.* **2007**, *104*, 15340−15345.
(35) Zheng, W.; Andrec, M.; Gallicchio, E.; Levy, R. M. Recovering Kinetics from a Simplified Protein Folding Model Using Replica Exchange Simulations: A Kinetic Network and Effective Stochastic Dynamics. *J. Phys. Chem. B* **2009**, *113*, 11702−11709.
(36) Zheng, W.; Gallicchio, E.; Deng, N.; Andrec, M.; Levy, R. M. Kinetic Network Study of the Diversity and Temperature Dependence of Trp-Cage Folding Pathways: Combining Transition Path Theory with Stochastic Simulations. *J. Phys. Chem. B* **2011**, *115*, 1512−1523.
(37) Ozkan, S. B.; Dill, K. A.; Bahar, I. Fast-Folding Protein Kinetics, Hidden Intermediates, and the Sequential Stabilization model. *Protein Sci.* **2002**, *11*, 1958−1970.
(38) Singhal, N.; Snow, C. D.; Pande, V. S. Using Path Sampling to Build Better Markovian State Models: Predicting the Folding Rate and Mechanism of a Tryptophan Zipper Beta Hairpin. *J. Chem. Phys.* **2004**, *121*, 415−425.
(39) Swope, W.; Pitera, J. W.; Suits, F. Describing Protein Folding Kinetics by Molecular Dynamics Simulations. 1. Theory. *J. Chem. Phys.* **2004**, *108*, 6571−6581.
(40) Sriraman, S.; Kevrekidis, I. G.; Hummer, G. Coarse Master Equation for Bayesian Analysis of Replica Molecular Dynamics Simulations. *J. Phys. Chem. B* **2005**, *109*, 6479−6484.
(41) Noe, F.; Krachtus, D.; Smith, J. C.; Fischer, S. Transition Networks for the Comprehensive Characterization of Complex Conformational Change in Proteins. *J. Chem. Theory Comput.* **2006**, *2*, 840−857.
(42) Sugita, Y.; Okamoto, Y. Replica-Exchange Molecular Dynamics Method for Protein Folding. *Chem. Phys. Lett.* **1999**, *314*, 141−151.
(43) Berezhkovskii, A.; Hummer, G.; Szabo, A. Reactive Flux and Folding Pathways in Network Models of Coarse-Grained Protein Dynamics. *J. Chem. Phys.* **2009**, *130*, 205102−205106.
(44) Gillespie, D. T. Exact Stochastic Simulation of Coupled Chemical Reactions. *J. Phys. Chem.* **1977**, *81*, 2340−2361.
(45) Levy, R. M.; Karplus, M.; McCammon, J. A. Increase of Carbon-13 NMR relaxation times in Proteins due to Picosecond Motional averaging. *J. Am. Chem. Soc.* **1981**, *103*, 994−996.
(46) Levy, R. M.; Karplus, M.; Wolynes, P. G. NMR Relaxation Parameters in Molecules with Internal Motion: Exact Langevin Trajectory Results Compared with Simplified Relaxation Models. *J. Am. Chem. Soc.* **1981**, *103*, 5998−6011.
(47) Lipari, G.; Szabo, A.; Levy, R. M. Protein Dynamics and NMR Relaxation: Comparison of Simulations with Experiment. *Nature* **1982**, *300*, 197−198.
(48) Levy, R. M.; Sheridan, R. P. Combined Effect of Restricted Rotational Diffusion Plus Jumps on Nuclear Magnetic Resonance and Fluorescence Probes of Aromatic Ring Motions in Proteins. *Biophys. J.* **1983**, *41*, 217−221.
(49) Wong, V.; Case, D. A. Evaluating Rotational Diffusion from Protein MD Simulations. *J. Phys. Chem. B* **2008**, *112*, 6013−6024.
(50) Showalter, S. A.; Bruschweiler, R. Validation of Molecular Dynamics Simulations of Biomolecules Using NMR Spin Relaxation as Benchmarks: Application to the AMBER99SB Force Field. *J. Chem. Theory Comput.* **2007**, *3*, 961−975.
(51) Peter, C.; Daura, X.; van Gunsteren, W. F. Calculation of NMR-Relaxation Parameters for Flexible Molecules from Molecular Dynamics Simulations. *J. Biomol. NMR* **2001**, *20*, 297−310.
(52) Fawzi, N. L.; Phillips, A. H.; Ruscio, J. Z.; Doucleff, M.; Wemmer, D. E.; Head-Gordon, T. Structure and Dynamics of the A$\beta_{21-30}$ Peptide from the Interplay of NMR Experiments and Molecular Simulations. *J. Am. Chem. Soc.* **2008**, *130*, 6145−6158.
(53) Xia, J.; Case, D. A. Sucrose in Aqueous Solution Revisited. Part 1:. Molecular Dynamics Simulations and Direct and Indirect Dipolar Coupling Analysis. *Biopolymers* **2012**, *97*, 276−288.
(54) Xia, J.; Case, D. A. Sucosae in Aqueous Solution Revisted. Part 2: Adaptively Biased Molecular Dynamics Simulations and Computational Analysis of NMR Relaxation. *Biopolymers* **2012**, *97*, 289−302.
(55) Chen, J. H.; Brooks, C. L.; Wright, P. E. Model-Free Analysis of Protein Dynamics: Assessment of Accuracy and Model Selection Protocols Based on Molecular Dynamics Simulation. *J. Biomol. NMR* **2004**, *29*, 243−257.
(56) Schneider, T. R.; Brunger, A. T.; Nilges, M. Influence of Internal Dynamics on Accuracy of Protein NMR Structures: Derivation of Realistic Model Distance Data from a Long Molecular Dynamics Trajectory. *J. Mol. Biol.* **1999**, *285*, 727−740.
(57) Noe, F.; Fischer, S. Transition Networks for Modeling the Kinetics of Conformational Change in Macromolecules. *Curr. Opin. Struct. Biol.* **2008**, *18*, 154−162.
(58) Pande, V. S.; Beauchamp, K.; Bowman, G. R. Everything You Wanted to Know about Markov State Models but were Afraid to Ask. *Methods* **2010**, *52*, 99−105.
(59) Prinz, J.-H.; Wu, H.; Sarich, M.; Keller, B.; Senne, M.; Held, M.; Chodera, J. D.; Schuette, C.; Noe, F. Markov Models of Molecular Kinetics: Generation and Validation. *J. Chem. Phys.* **2011**, *134*, 174105−174127.
(60) Yang, S.; Banavali, N. K.; Roux, B. Mapping the Conformational Transition in Src Activation by Cumulating the Information from Multipe Molecular Dynamics Trajectories. *Proc. Natl. Acad. Sci. U.S.A.* **2009**, *106*, 3776−3781.
(61) Da, L.-T.; Wang, D.; Huang, X. Dynamics of Pyrophosphate Ion Release and Its Coupled Trigger Loop Motion from Closed to Open State in RNA Polymerase II. *J. Am. Chem. Soc.* **2012**, *134*, 2399−2406.
(62) Lane, T. J.; Bowman, G. R.; Beauchamp, K.; Voelz, V. A.; Pande, V. S. Markov State Model Reveals Folding and Functional Dynamics in Ultra-Long MD Trajectories. *J. Am. Chem. Soc.* **2011**, *133*, 18413−18419.
(63) Buchete, N.-V.; Hummer, G. Coarse Master Equations for Peptide Folding Dynamics. *J. Phys. Chem. B* **2008**, *112*, 6057−6069.
(64) Buch, I.; Giorgino, T.; De Fabritiis, G. Complete Reconstruction of an Enzyme Inhibitor Binding Process by Molecular Dynamics Simulations. *Proc. Natl. Acad. Sci. U.S.A.* **2011**, *108*, 10184−10189.
(65) Fischer, S.; Karplus, M. Conjugate Peak Refinement—an Algorithm for Finding Reaction Paths and Accurate Transition-States in Systems with Many Degrees Freedom. *Chem. Phys. Lett.* **1992**, *194*, 252−261.
(66) Noe, F.; Schuette, C.; Vanden-Eijnden, E.; Reich, L.; Weikl, T. R. Constructing the equilibrium ensemble of folding pathways from short off-equilibrium simulations. *Proc. Natl. Acad. Sci. U.S.A.* **2009**, *106*, 19011−19016.
(67) Chodera, J. D.; Swope, W. C.; Pitera, J. W.; Dill, K. A. Long-Time Protein Folding Dynamics from Short-Time Molecular Dynamics Simulations. *Multiscale Model Simul.* **2006**, *5*, 1214−1226.
(68) Bacallado, S.; Chodera, J. D.; Pande, V. Bayesian Comparison of Markov Models of Molecular Dynamics with Detailed Balance Constraint. *J. Chem. Phys.* **2009**, *131*, 045106−045115.
(69) Noe, F. Probability Distributions of Molecular Observables Computed from Markov Models. *J. Chem. Phys.* **2008**, *128*, 244103−244115.
(70) Singhal, N.; Pande, V. S. Error Analysis and Efficient Sampling in Markovian State Models for Molecular Dynamics. *J. Chem. Phys.* **2005**, *123*, 204909−204921.
(71) Banks, J. L.; Beard, H. S.; Cao, Y.; Cho, A. E.; Damm, W.; Farid, R.; Felts, A. K.; Halgren, T. A.; Mainz, D. T.; Maple, J. R.; et al. Integrated Modeling Program, Applied Chemical Theory (IMPACT). *J. Comput. Chem.* **2005**, *26*, 1752−1780.
(72) Jorgensen, W. L.; Maxwell, D. S.; TiradoRives, J. Development and Testing of the OPLS All-Atom Force Field on Conformational Energetics and Properties of Organic Liquids. *J. Am. Chem. Soc.* **1996**, *118*, 11225−11236.

(73) Gallicchio, E.; Levy, R. M. AGBNP: An Analytic Implicit Solvent Model Suitable for Molecular Dynamics Simulations and High-Resolution Modeling. *J. Comput. Chem.* **2004**, *25*, 479−499.
(74) Gallicchio, E.; Paris, K.; Levy, R. M. The AGBNP2 Implicit Solvation Model. *J. Chem. Theory Comput.* **2009**, *5*, 2544−2564.
(75) Gallicchio, E.; Andrec, M.; Felts, A. K.; Levy, R. M. Temperature Weighted Histogram Analysis Method, Replica Exchange, and Transition Paths. *J. Phys. Chem. B* **2005**, *109*, 6722−6731.
(76) Pearlman, D. A.; Kollman, P. A. Evaluating the Assumptions Underlying Force-Field Development and Application Using Free-Energy Conformational Maps for Nucleosides. *J. Am. Chem. Soc.* **1991**, *113*, 7167−7177.
(77) Favro, L. D. Theory of the Rotational Brownian Motion of a Free Rigid Body. *Phys. Rev.* **1960**, *119*, 53−62.
(78) Woessner, D. E. Nuclear Spin Relaxation in Ellipsoids Undergoing Rotational Brownian Motion. *J. Chem. Phys.* **1962**, *37*, 647−654.
(79) Woessner, D. E.; Snowden, B. S.; Meyer, G. H. Nuclear Spin-Lattice Relaxation in Axially Symmetric Ellipsoids with Internal Motion. *J. Chem. Phys.* **1969**, *50*, 719−721.
(80) Wallach, D. Effect of Internal Rotation on Angular Correlation Functions. *J. Chem. Phys.* **1967**, *47*, 5258−5268.
(81) Wittebort, R. J.; Szabo, A. Theory of NMR Relaxation in Macromolecules: Restricted Diffusion and Jump models for Multiple Internal Rotations in Amino Acide Side Chains. *J. Chem. Phys.* **1978**, *69*, 1722−1736.
(82) Wong, V.; Case, D. A.; Szabo, A. Influence of the Coupling of Interdomain and Overall Motions on NMR Relaxation. *Proc. Natl. Acad. Sci. U.S.A.* **2009**, *106*, 11016−11021.
(83) Ryabov, Y.; Clore, G. M.; Schwieters, C. D. Coupling between Internal Dynamics and Rotational Diffusion in the Presence of Exchange between Discrete Molecular Conformations. *J. Chem. Phys.* **2012**, *136*, 034108−034112.
(84) Ryabov, Y. E.; Fushman, D. A Model of Interdomain Mobility in a Multidomain Protein. *J. Am. Chem. Soc.* **2007**, *129*, 3315−3327.
(85) Prompers, J. J.; Bruschweiler, R. General Framework for Studying the Dynamics of Folded and Nonfolded Proteins by NMR Relaxation Spectroscopy and MD Simulation. *J. Am. Chem. Soc.* **2002**, *124*, 4522−4534.
(86) Perryman, A. L.; Lin, J. H.; McCammon, J. A. HIV-1 Protease Molecular Dynamics of a Wide-Type and of the V82F/I84V Mutant: Possible Contributions to Drug Resistance and a Potential New Target Site for Drugs. *Protein Sci.* **2004**, *13*, 1108−1123.
(87) Galiano, L.; Ding, F.; Veloro, A. M.; Blackburn, M. E.; Simmerling, C.; Fanucci, G. E. Drug Pressure Selected Mutations in HIV-1 Protease Alter Flap Conformations. *J. Am. Chem. Soc.* **2009**, *131*, 430−431.
(88) Kear, J. L.; Blackburn, M. E.; Veloro, A. M.; Dunn, B. M.; Fanucci, G. E. Subtype Polymorphisms among HIV-1 Protease Variants Confer Altered Flap Conformations and Flexibility. *J. Am. Chem. Soc.* **2009**, *131*, 14650−14651.
(89) Blackburn, M. E.; Veloro, A. M.; Fanucci, G. E. Monitoring Inhibitor-Induced Conformational Population Shifts in HIV-1 Protease by Pulsed EPR Spectroscopy. *Biochemistry* **2009**, *48*, 8765−8767.
(90) Cai, Y.; Yilmaz, N. K.; Myint, W.; Ishima, R.; Schiffer, C. A. Differential Flap Dynamics in Wild-Type and a Drug Resistant Variant of HIV-1 Protease Revealed by Molecular Dynamics and NMR Relaxation. *J. Chem. Theory Comput.* **2012**, *8*, 3452−3462.
(91) Marinelli, F.; Pietrucci, F.; Laio, A.; Piana, S. A Kinetic Model of Trp-Cage Folding from Multiple Biased Molecular Dynamics Simulations. *PLOS Comput. Biol.* **2009**, *5*, e1000452.